

## Rab4 Is an Essential Regulator of Lysosomal Trafficking in Trypanosomes\*

Received for publication, June 29, 2004

Published, JBC Papers in Press, July 28, 2004, DOI 10.1074/jbc.M407271200

Belinda S. Hall, Arun Pal‡, David Goulding, and Mark C. Field§

From the Department of Biological Sciences, Imperial College, London SW7 2AY, United Kingdom

**Rapid endocytosis and recycling of surface proteins are important processes common to most nucleated eukaryotic cells. The best characterized membrane recycling routes are mediated by the small GTPases Rab4 and Rab11, but the precise roles that these pathways play have not been fully elucidated. The protozoan *Trypanosoma brucei* has a highly developed endocytic system that is similar to that found in metazoans, albeit with an accelerated rate of membrane turnover. We have used this organism to investigate the function of the trypanosome orthologue of Rab4 (TbRAB4) by a combination of RNA interference, microscopy, and quantitative trafficking assays. RNA interference-mediated suppression of TbRAB4 expression inhibited the growth of trypanosomes without affecting receptor-mediated endocytosis or ligand recycling. Ultrastructural analysis indicated a major defect in membrane transport events. The accumulation of fluorescent dextran, a fluid-phase marker, was blocked in cells lacking TbRAB4 protein. Since most fluid-phase markers are transported to the lysosome in *T. brucei*, the effects of TbRAB4 RNA interference on lysosomal function were investigated. By immunofluorescence, the major lysosomal protein p67 became progressively dispersed in cells lacking the TbRAB4 protein. Pulse-chase analysis demonstrated that initial proteolytic cleavage and glycan processing of p67 were unaffected but that cells failed to accumulate the later p67 proteolyzed products associated with the lysosome. To confirm the role of TbRAB4 in lysosomal trafficking, a constitutively active mutant, TbRAB4<sup>QL</sup>, was expressed. TbRAB4<sup>QL</sup> was closely associated with an enlarged multivesicular body that contained p67. In addition, cells expressing TbRAB4<sup>QL</sup> showed increased fluid-phase uptake when compared with the parental line. Taken together, these data suggest that TbRAB4 is involved in regulation of fluid-phase traffic to the lysosome in *T. brucei* but not in receptor-mediated endocytosis or recycling. These data have implications for the role of Rab4 in other cell systems.**

Endocytic and recycling pathways mediate many processes including nutrient uptake, membrane homeostasis, receptor repair mechanisms, and signal transduction (1). Several recycling routes have been described in higher eukaryotes, but the best understood of these are the Rab4- and Rab11-dependent recycling pathways. Rab family proteins are a subgroup of the

Ras family small GTPases that specialize in regulation of membrane trafficking (2). Mammalian Rab4 is implicated in recycling of many surface proteins including transferrin receptor, G-protein-coupled receptors, integrins, and surfactant protein A (3–7). Rab4 shares effector proteins with both Rab5 and Rab11, and sequential interactions provide direction to the movement of cargo through endocytic and recycling systems (4, 8–11). Rab4 also controls Ca<sup>2+</sup>-dependent exocytosis in platelets and insulin-stimulated translocation of GLUT4 from internal vesicles to the cell surface (12, 13). However, there is also some evidence for involvement of Rab4 in degradative trafficking (14, 15).

*Trypanosoma brucei* is a protozoan parasite that contains a sophisticated and highly active endocytic system (16). The plasma membrane of *T. brucei* is dominated by  $1 \times 10^7$  copies of the variant surface glycoprotein (VSG),<sup>1</sup> which are attached to the membrane via a glycosylphosphatidylinositol anchor. VSG constitutes ~90% of surface protein and is subject to continuous turnover (16–18). *T. brucei* exhibits one of the fastest known rates of endocytosis and recycling despite all import and export being limited to the flagellar pocket, an invagination at the posterior of the cell where the flagellum enters the cytoplasm, representing ~5% of the total plasma membrane (19). This high rate of endocytic activity may be important in removal of surface immune effectors including antibodies (20), but inhibition of endocytosis is rapidly lethal even in the absence of immune effectors, suggesting an essential role in membrane homeostasis (21–23).

The intracellular routes taken by internalized cargo in trypanosomes have been partially resolved. VSG is endocytosed into class I clathrin-coated vesicles and transported to a tubular endosome network, along with fluid-phase cargo (17). The latter exits the endosome via a second clathrin-dependent step mediated by class II clathrin-coated vesicles and is transported to the lysosome (18). The majority of VSG is recycled directly back to the surface, but a portion is transported to the late endosome before recycling, apparently without entering the lysosome. The transferrin receptor takes a similar route to VSG (24), but kinetic analysis indicates differences in the intracellular transport of these two molecules (20). Transferrin is efficiently degraded within the trypanosome and was originally reported to be transported to the lysosome (25). More recent data suggest that the majority of transferrin is recycled, albeit extensively degraded (20), indicating the presence of an extensive proteolysis system within the trypanosome recycling system.

Trypanosome orthologues of Rab proteins controlling endocytosis and recycling pathways are present in the genome (26). Two TbRAB5 homologues, TbRAB5A and TbRAB5B, have been

\* This work was supported by a program grant from the Wellcome Trust (to M. C. F.). The costs of publication of this article were defrayed in part by the payment of page charges. This article must therefore be hereby marked "advertisement" in accordance with 18 U.S.C. Section 1734 solely to indicate this fact.

‡ Present address: Max-Planck-Institute of Molecular Cell Biology and Genetics, Pfotenhauerstrasse 110, 01307 Dresden, Germany.

§ To whom correspondence should be addressed. Tel.: 020-7594-5277; E-mail: mfield@mac.com.

<sup>1</sup> The abbreviations used are: VSG, variant surface glycoprotein; BSF, bloodstream form; BiP, binding protein; Con A, *Canavalia ensiformis* lectin concanavalin A; DAPI, 4',6-Diamidino-2-phenylindole; RNAi, RNA interference; PBS, phosphate-buffered saline; BSA, bovine serum albumin; WT, wild type.

characterized in some detail and are required for early endocytosis (23, 27, 28). Moreover, TbRAB5A is associated with internalized glycosylphosphatidylinositol-anchored proteins such as VSG and ESAG6/7, but TbRAB5B colocalizes with the invariant transmembrane protein ISG<sub>100</sub>, suggesting the presence of at least two distinct endocytic pathways (28). Both appear to have a role in clathrin-mediated endocytosis, and RNAi of either isoform blocks endocytosis (23). Further, all available evidence suggests that the Rab11 homologue, TbRAB11, is responsible for recycling of VSG and the transferrin receptor, as well as recycling of degraded transferrin and antibodies (17, 18, 20, 24). The roles of the two TbRAB5 isoforms and TbRAB11 are therefore comparable with their mammalian orthologues.

Previous work from this laboratory demonstrated that TbRAB4, the *T. brucei* orthologue of mammalian Rab4, is a constitutively expressed protein located at the endocytic pathway (27), but analysis of cells expressing mutant forms of TbRAB4 has been unable to ascribe a clear function in either endocytosis or recycling (20). Here we have examined TbRAB4 function using RNA interference and demonstrate that this GTPase has a highly specialized role in transport of fluid-phase cargo toward the lysosome in trypanosomes.

#### MATERIALS AND METHODS

**Cell Culture**—The bloodstream form trypanosome (BSF) lines *T. brucei* Lister 427 and BSF 90-13 were maintained in HMI 9 medium supplemented with 10% tetracycline-free fetal bovine serum (Autogen Bioclear). BSF 90-13 cells were cultured in the continuous presence of 5  $\mu\text{g ml}^{-1}$  hygromycin B (Sigma) and 2.5  $\mu\text{g ml}^{-1}$  Geneticin (Sigma) to maintain the T7-responsive phenotype. For growth curves, triplicate cultures were initiated at  $5 \times 10^4$  cells  $\text{ml}^{-1}$ , and BSF cell numbers were determined using a Z2 Coulter counter (Beckman Coulter).

**Recombinant DNA Manipulations and Transfection**—TbRAB4<sup>WT</sup> was amplified from cDNA using the primers 5'-CGGAAAGCTTACC-ATGTCAGAGAG-3' and 5'-TTTGGATCCAATACCTAACAAGC-3'. Underlined bases represent HindIII and BamHI restriction sites, respectively. The TbRAB4<sup>QL</sup> mutant was prepared using the primers 5'-CCGGTCTAGAAAGATACAAATCAG-3' and 5'-CTGATTTGTATCTTCT-AGACCGGC-3'. PCR products were digested with BamHI and HindIII and inserted into pXS19 vector (28). For RNAi experiments, the entire TbRAB4 open reading frame was excised from pSX519-TbRAB4<sup>WT</sup> using BamHI and HindIII and inserted into p2T7<sup>Ti</sup> (29). The pXS19-TbRAB4<sup>QL</sup> construct was transfected by electroporation into Lister 427 strain BSF, and transfectants were selected using 2.5  $\mu\text{g ml}^{-1}$  Geneticin (Sigma), whereas p2T7<sup>Ti</sup>-TbRAB4 was introduced into the tetracycline-responsive line, BSF 90-13, and cells were cultured for 6 h before the addition of 2.5  $\mu\text{g ml}^{-1}$  phleomycin (Sigma). After 7 days of culture in the presence of selective drug, cells were cloned by limiting dilution. Clones were maintained thereafter in the presence of phleomycin or Geneticin.

**Antibodies**—The TbRAB4 open reading frame was amplified with the primers 5'-CGGAGGATCCAACCATGTCAGAGAGATATC-3' and 5'-GTGGAATTCAAATACCTAACAAGCACACG-3'. The product was digested with BamHI and EcoRI (underlined) and inserted into pGEX-3X (Amersham Biosciences). Polyclonal murine and rabbit antibodies were raised against affinity-purified TbRAB4-GST fusion protein using RIBI (Sigma) as adjuvant (at least four immunizations spaced over a period of 4 months). Antibodies were affinity-purified on CNBr-Sepharose-immobilized TbRAB4-GST. Anti-TbRAB11 antibodies have been described elsewhere (24). Polyclonal rabbit anti-BiP antibodies and monoclonal anti-p67 antibody mAb280 were a kind gift from J. Bangs (30, 31).

**Western Blot Analysis**—Cells were washed once in PBS and resuspended in SDS sample buffer and boiled. Lysates were loaded onto 12% SDS-PAGE gels at  $1 \times 10^7$  cell equivalents/lane. After separation, proteins were transferred onto Hybond nitrocellulose membranes (Amersham Biosciences). Membranes were blocked with PBS, 5% milk, 0.1% Tween 20 for 1 h at room temperature and then incubated overnight at 4 °C in the presence of affinity-purified rabbit anti-TbRAB4 or rabbit anti-TbRAB11 at a concentration of  $\sim 1 \mu\text{g ml}^{-1}$  in blocking buffer (24). Membranes were washed in PBS, 0.1% Tween 20 and then incubated with peroxidase-conjugated goat anti-rabbit IgG (Sigma) for 1 h. Bound antibody was visualized by enhanced chemiluminescence. To ensure equality of loading, membranes were stripped and reprobed

with antibody to TbBiP (31). Where appropriate, signal intensity was quantified using NIH Image software.

**Immunofluorescence**—Cells were fixed in 4% paraformaldehyde, adhered to poly-L-lysine slides (Sigma), and permeabilized with 0.1% Triton X-100. Slides were blocked with 10% goat serum in PBS. For staining of TbRAB4, slides were incubated overnight at 4 °C with affinity-purified rabbit or mouse anti-TbRAB4 antibodies at 1  $\mu\text{g ml}^{-1}$  in blocking buffer containing 0.02% sodium azide. All other primary antibody incubations were carried out for 1 h at room temperature. After washing with PBS, slides were incubated with Texas Red-conjugated goat anti-rabbit or Alexa Fluor 488 goat anti-mouse IgG (Molecular Probes) for 1 h at room temperature. Slides were washed and mounted with Vectashield containing DAPI (Vector Laboratories). Cells were examined under a Nikon Eclipse E600 microscope, and images were captured using a Photometrix Coolsnap-FX camera controlled with Metamorph (Universal Imaging Corp.) and assembled in PhotoShop 7.0.1 (Adobe Inc.).

**Electron Microscopy**—For transmission electron microscopy, cells were fixed in suspension by adding chilled 5% glutaraldehyde and 8% paraformaldehyde (Sigma) in PBS in a 1:1 ratio to the growth medium containing trypanosomes. Cells were fixed on ice for 10 min and centrifuged at 10,000 rpm for 5 min in 2-ml microcentrifuge tubes, and the supernatant was carefully replaced with fresh fixative for a further 50 min without disturbing the pellet, rinsed in 0.1 M sodium cacodylate, and post-fixed in 1% osmium tetroxide in the same buffer at room temperature for 1 h. After rinsing in buffer, cells were then dehydrated in an ethanol series, adding 1% uranyl acetate at the 30% stage, followed by propylene oxide, and then embedded in Epon/Araldite 502 and finally polymerized at 60 °C for 48 h. Sections were cut on a Leica Ultracut-T ultramicrotome at 70 nm using a diamond knife, contrasted with uranyl acetate and lead citrate and examined on a Philips CM100 transmission electron microscope.

**Transferrin Endocytosis and Recycling**—Bovine holo-transferrin (Sigma) was iodinated using IodoBeads reagent (Pierce) following the manufacturer's instructions. Assays were carried out as described in Ref. 28. Briefly, expression of double-stranded RNA corresponding to TbRAB4 in p2T7<sup>Ti</sup>-TbRAB4 cells was induced for 24 h with 1  $\mu\text{g ml}^{-1}$  tetracycline, whereas parental and TbRAB4<sup>QL</sup> cells were harvested in mid-log phase. Cells were washed twice with serum-free HMI 9 containing 1% BSA (Sigma) (SF/HMI 9). Washed cells were incubated at 37 °C for 30 min at a concentration of  $1 - 2 \times 10^7$  cells  $\text{ml}^{-1}$ , and then <sup>125</sup>I-labeled transferrin was added (typically  $\sim 2 \mu\text{g}$  at a specific activity of  $3 \times 10^6$  cpm  $\mu\text{g}^{-1}$ ). Triplicate 500- $\mu\text{l}$  samples of cells were incubated at 4 or 37 °C for various times. Nonspecific binding controls included cold transferrin at a concentration of 600  $\mu\text{g ml}^{-1}$ . Accumulation was stopped by the addition of 500  $\mu\text{l}$  of cold SF/HMI9 containing 600  $\mu\text{g ml}^{-1}$  transferrin. Cells were washed three times in ice-cold PBS, 0.05% BSA and resuspended in 200  $\mu\text{l}$  of PBS. The accumulation of <sup>125</sup>I was measured in a  $\gamma$ -counter (Beckman Coulter). For recycling of transferrin degradative products, cells were pulsed for 40 min with transferrin and washed in PBS/BSA as described above and then resuspended to a final concentration of  $2 \times 10^7$  cells  $\text{ml}^{-1}$  in complete HMI9. Cells were incubated for 20 min at 37° or 4 °C and then centrifuged for 1 min at  $13,000 \times g$  at 4 °C. Radioactivity in supernatants and pellets was determined as described.

**Endocytosis of Concanavalin A (Con A)**—Mid-log phase cells were harvested and washed once in serum-free HMI 9 medium containing 1% BSA. Cells were resuspended in HMI 9 + BSA at a concentration of  $1 \times 10^7 \text{ ml}^{-1}$  and incubated at 4 or 37 °C for 20 min. Biotinylated Con A (100  $\mu\text{g ml}^{-1}$ ) (Vectalabs) was added, and the cells were incubated for a further 30 min. Uptake was stopped by placing the cells on ice. Labeled cells were washed in HMI 9 + BSA at 4 °C and then fixed and adhered to slides as described above. Slides were either mounted immediately or counterstained with antibody. Biotinylated Con A was detected by incubating for 1 h at room temperature with Texas Red-conjugated streptavidin (Vectalabs).

**Fluid-phase Uptake**—Cells were induced for 24 h with tetracycline or harvested directly from mid-log phase cultures and resuspended at a concentration of  $5 \times 10^8 \text{ ml}^{-1}$  in 50- $\mu\text{l}$  aliquots of fresh complete medium. Alexa Fluor 488-labeled dextran 10000 (Molecular Probes) was added to a concentration of 5 mg  $\text{ml}^{-1}$ . Cells were incubated for various times, and accumulation was stopped by the addition of 1 ml of cold medium. Cells were washed and then fixed in 4% paraformaldehyde for 1 h before mounting onto poly-L-lysine slides (Sigma). Fluorescence was quantified using Metamorph imaging software.

**Pulse-chase Analysis of p67 Processing**—Processing of p67 was followed as described in Ref. 32. p2t7<sup>Ti</sup>-TbRAB4 cells were incubated for 24 h in the presence of 1  $\mu\text{g ml}^{-1}$  tetracycline, harvested, and washed

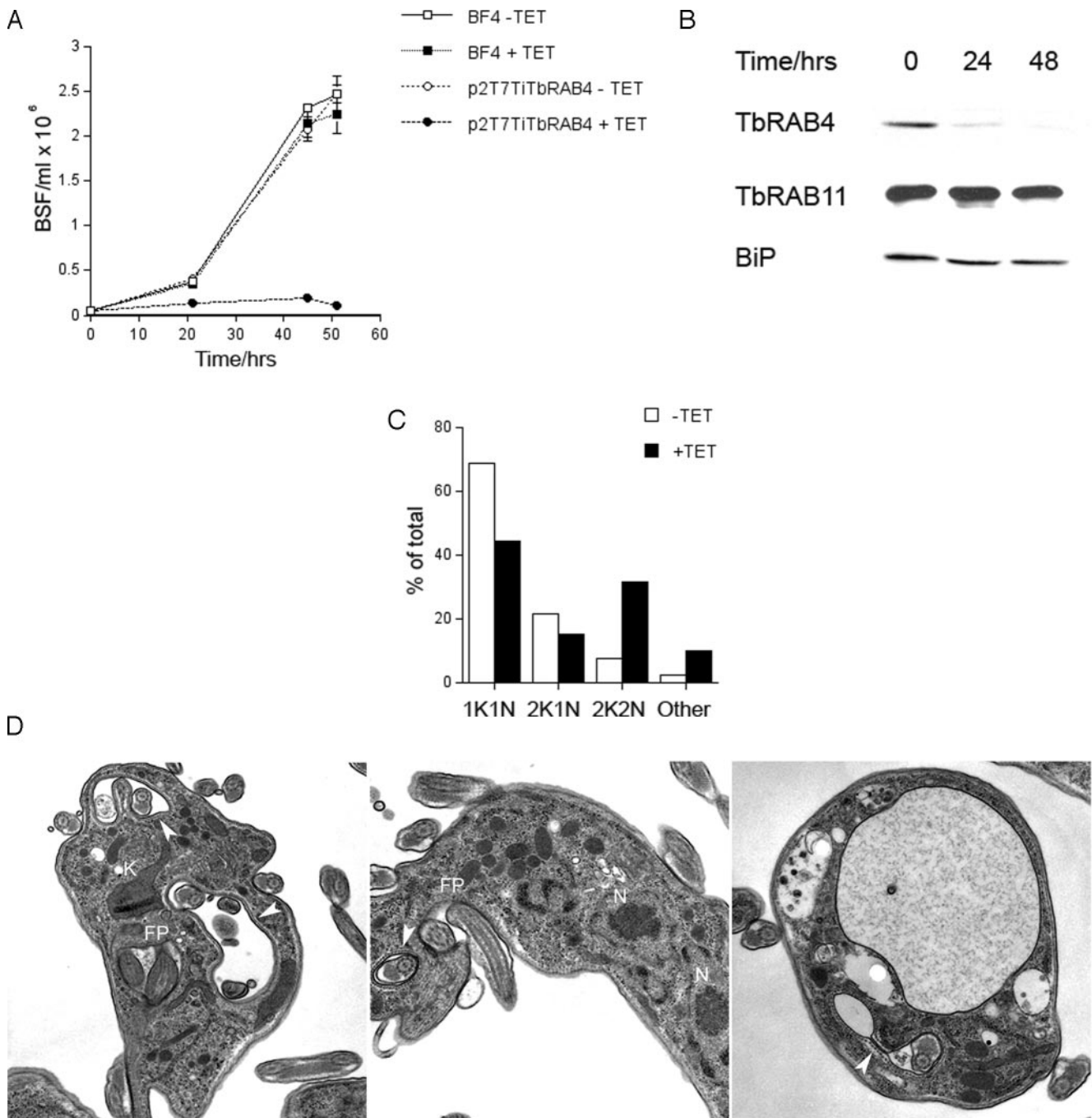


**FIG. 1. TbRAB4 RNAi inhibits cell growth of bloodstream form *T. brucei*.** *A*, growth rates for parental BF4 cells (squares) and p2T7TiTbRAB4 cells (circles) in the absence (open) and presence (closed) of tetracycline (TET). Each data point represents the mean of triplicate samples  $\pm$  S.E. The data are typical of multiple repeated experiments. *B*, Western blot of TbRAB4 and TbRAB11 in p2T7TiTbRAB4 cells exposed to tetracycline for 0, 24, and 48 h. Each lane contains  $10^7$  cell equivalents. Anti-trypanosome BiP was used as a loading control. *C*, p2T7TiTbRAB4 cells were cultured for 24 h with tetracycline, fixed with 4% paraformaldehyde, and stained with DAPI to determine the position in the cell cycle. The numbers of nuclei and kinetoplasts per cell were counted for at least 150 cells for induced (closed bars) and uninduced (open bars) cultures. The data presented are representative of duplicate experiments. *D*, electron micrographs of p2T7TiTbRAB4 cells exposed to tetracycline for 24 h. Arrows indicate microtubules around surface membrane invaginations. FP, flagellar pocket; N, nucleus; K, kinetoplast.

twice in Met/Cys-free Dulbecco's modified Eagle's medium (Sigma) and then resuspended to a concentration of  $2 \times 10^7$  ml<sup>-1</sup> in 500  $\mu$ l of Met/Cys-free Dulbecco's modified Eagle's medium supplemented with dialyzed fetal bovine serum and incubated for 20 min at 37  $^{\circ}$ C. <sup>35</sup>S-labeled Promix (Amersham Biosciences) was added at 200  $\mu$ Ci ml<sup>-1</sup>, and cells were incubated for 15 min at 37  $^{\circ}$ C. A chase was initiated with the addition of 4.5 ml of complete HMI 9 medium, and 1-ml samples were withdrawn at different time points and placed on ice. Cells were washed once in PBS and then lysed with 1 ml of ice-cold radioimmune precipitation buffer (25 mM Tris-Cl, pH 7.5, 150 mM NaCl, 1% Nonidet P-40, 0.5% sodium deoxycholate, 0.1% SDS, and complete protease inhibitor mixture (Roche Applied Science)). Lysates were precleared

and then incubated for 1 h at 4  $^{\circ}$ C with anti-p67 mAb280 and then incubated for a further 1 h with 10  $\mu$ l of protein A-Sepharose beads (Amersham Biosciences). After washing, immunoprecipitates were resuspended in 40  $\mu$ l of loading buffer and run on 12% SDS-PAGE gels. Fixed, stained gels were incubated for 1 h in En<sup>3</sup>Hance (PerkinElmer Life Sciences), dried, and autoradiographed. The intensity of metabolically labeled protein bands was quantified using the NIH Image program.

## RESULTS

*TbRAB4 Is Essential in Bloodstream Form *T. brucei**—Previous studies on TbRAB4 function used overexpression of domi-

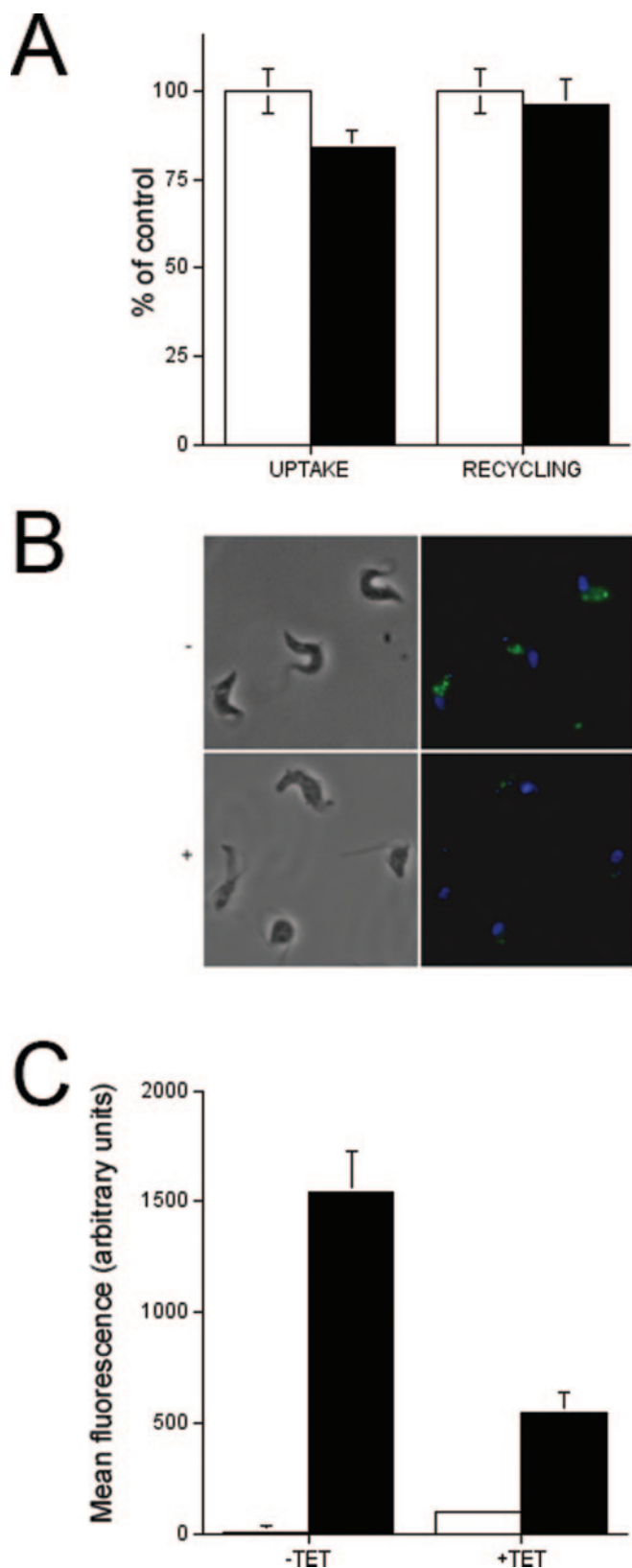


**FIG. 2. TbRAB4 RNAi specifically inhibits accumulation of fluid-phase cargo.** *A*, uptake and recycling of transferrin are unaffected by TbRAB4 RNAi. p2T7<sup>Tb</sup>TbRAB4 cells were induced for 24 h with tetracycline (closed bars) and then assayed for the uptake of <sup>125</sup>I-transferrin for 40 min. Specific pellet-associated radioactivity was determined. Data are presented as a percentage of uninduced controls (open bars). Recycling was determined by washing pulse-labeled cells and reincubation at 37 °C. Data were calculated as a percentage of the total label in the supernatant after 20 min when compared with background in supernatants of cells incubated at 4 °C and are presented as

nant negative and dominant positive forms of the protein (20). These analyses resulted in no detectable phenotype with the assays available. In this study, expression of the TbRAB4 protein was suppressed by RNA interference (Fig. 1). The induction of expression of double-stranded TbRAB4 RNA with tetracycline led to a rapid decrease in TbRAB4 expression such that the protein was essentially undetectable by 48 h after induction (Fig. 1*B*). Suppression of TbRAB4 expression was accompanied by a significant inhibition of cell growth (Fig. 1*A*). Similar results were obtained with several independently generated cloned lines. TbRAB4 RNAi had no effect on cellular levels of other Rab proteins, specifically TbRAB11 (Fig. 1*B*) or TbRAB5A (not shown).

Examination of DAPI-stained cells revealed an increase in the proportion of cells with two nuclei and two kinetoplasts, suggesting a block in cell division but not in mitosis (Fig. 1*C*). The effect of TbRAB4 RNAi was not as rapid or severe as that triggered by depletion of clathrin or TbRAB5A (21, 23), but after 24 h of incubation with tetracycline, multiple abnormal cells were present in cultures (Fig. 1*D*). A variety of ultrastructural defects were visible by electron microscopy, the most prominent of which was the appearance of membrane invaginations, distinguishable from the flagellar pocket by the presence of subpellicular microtubules, suggesting that these structures derived from the plasma membrane. Interestingly, the enlargement of the flagellar pocket characteristic of a general inhibition of endocytosis (21–23) was only apparent in ~5% of cells at this stage (Fig. 1*D*), suggesting that TbRAB4 is not directly involved in early endocytosis in *T. brucei*. Overall, these data suggest that a defect in membrane dynamics is associated with suppression of TbRAB4.

*Endocytosis and Recycling of Transferrin Are Normal, but Accumulation of a Fluid-phase Marker Is Inhibited by TbRAB4 RNAi*—The uptake of iron-bound transferrin is essential to the survival of bloodstream form *T. brucei* (33). Results from previous work indicated that transferrin is subject to very rapid turnover regulated by TbRAB11 but not TbRAB4 (20). However, in this study, a single round of transferrin uptake, degradation, and recycling was monitored, which may not be sufficiently sensitive to detect a relatively minor role for TbRAB4. Further, expression of a dominant negative mutant GTPase as used in the earlier experiments is not equivalent to RNAi-mediated ablation of TbRAB4 expression. Therefore, the effect of TbRAB4 RNAi on bulk transferrin accumulation and recycling was examined. Cells were induced and then allowed to accumulate <sup>125</sup>I-transferrin for 40 min. To monitor recycling, cells were then washed and returned to medium for 20 min, and <sup>125</sup>I recovery in the supernatant was monitored. No significant effect was found for either the accumulation of <sup>125</sup>I-transferrin or the recycling of previously internalized label into the supernatant ( $p > 0.10$ ) (Fig. 2). Under the same conditions, RNAi of TbRAB5 isoforms reduces transferrin endocytosis (23), and TbRAB11 RNAi causes an almost complete inhibition of

a percentage of the uninduced controls. All data represent the mean of triplicate samples  $\pm$  S.E. and are typical of multiple repeated experiments. *B*, inhibition of fluid-phase uptake in TbRAB4 RNAi. p2T7<sup>Tb</sup>TbRAB4 cells were induced for 24 h with (+) or without (–) tetracycline and then incubated for 30 min with Alexa Fluor 488 dextran 10000 (green). Cells were fixed in 4% paraformaldehyde, adhered to poly-L-lysine slides, counterstained with DAPI (blue), and examined immediately. *C*, quantitation of fluid-phase uptake. The accumulation of fluorophore in uninduced (–TET) and induced p2T7<sup>Tb</sup>TbRAB4 cells (+TET) labeled at 4 °C (open bars) or 37 °C (closed bars) as described above was measured using Metamorph Imaging software. Data represent the signal above background for at least 50 cells  $\pm$  S.E. and are typical of triplicate experiments.

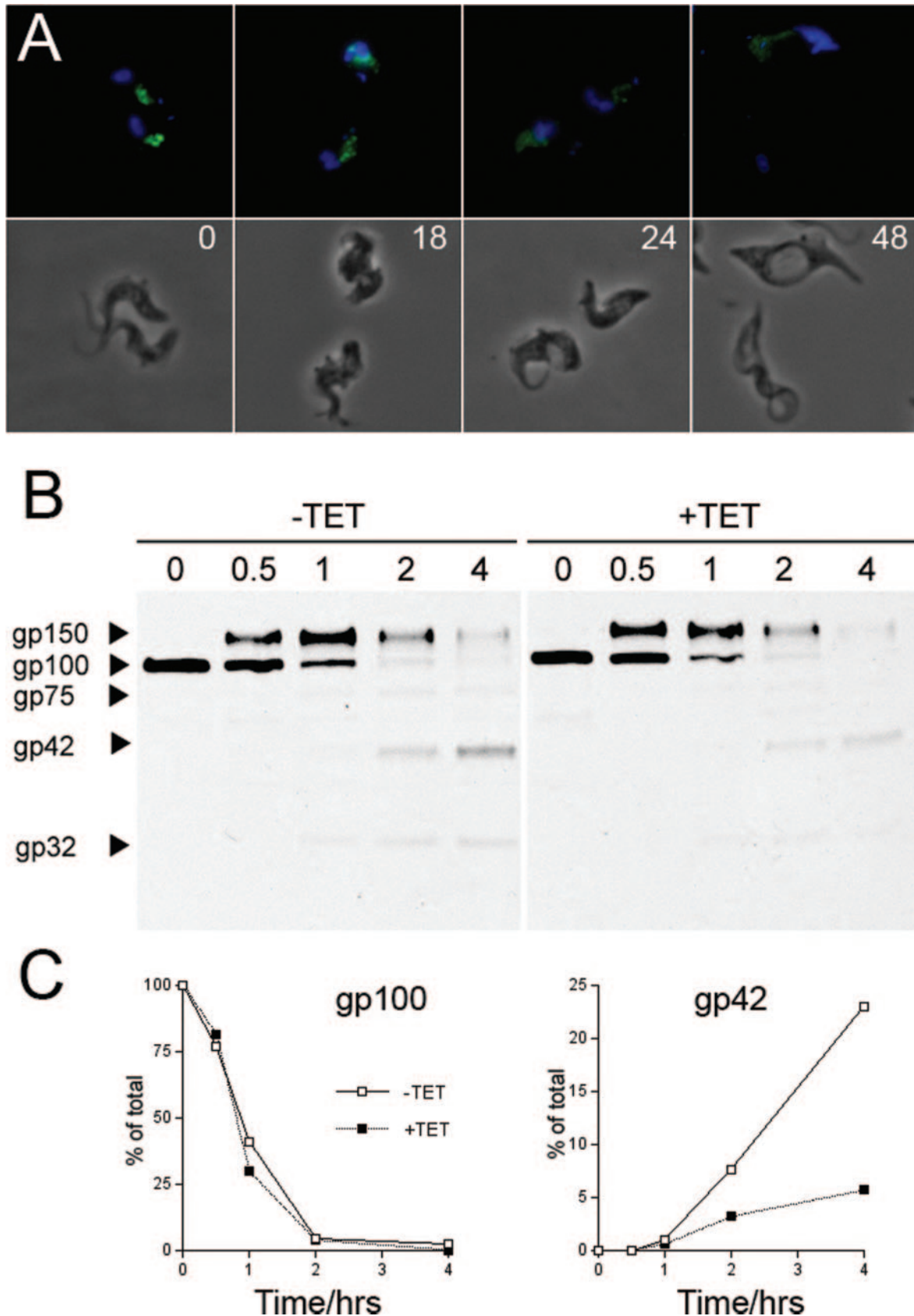


**FIG. 3. Disruption of p67 labeling and processing in TbRAB4 RNAi.** *A*, loss of p67-positive compartments in TbRAB4 RNAi. p2T7<sup>Tb</sup>-TbRAB4 cells were incubated for 0–48 h as indicated in the presence of 1  $\mu\text{g ml}^{-1}$  tetracycline and then fixed and stained for p67 with mAb280 (green) as described under “Materials and Methods.” Cells were counterstained with DAPI to show the position of the kinetoplast and nucleus. *B*, reduced accumulation of p67 proteolytic fragments in TbRAB4 RNAi. p2T7<sup>Tb</sup>-TbRAB4 cells were incubated for 24 h in the presence of 1  $\mu\text{g ml}^{-1}$  tetracycline (TET), pulse-labeled with [<sup>35</sup>S]methionine, and then cultured for times up to 4 h. Cells were lysed, and p67 was immunoprecipitated with mAb280. Each lane contains  $5 \times 10^6$  cell equivalents. Arrows indicate the different molecular weight fragments produced during p67 processing (see Ref. 32). *C*, quantitation of band intensity of gp100 precursor and gp42 proteolytic fragments was done using NIH Image software. Results are presented as a percentage of the initial gp100 intensity. Similar results were obtained in duplicate experiments.

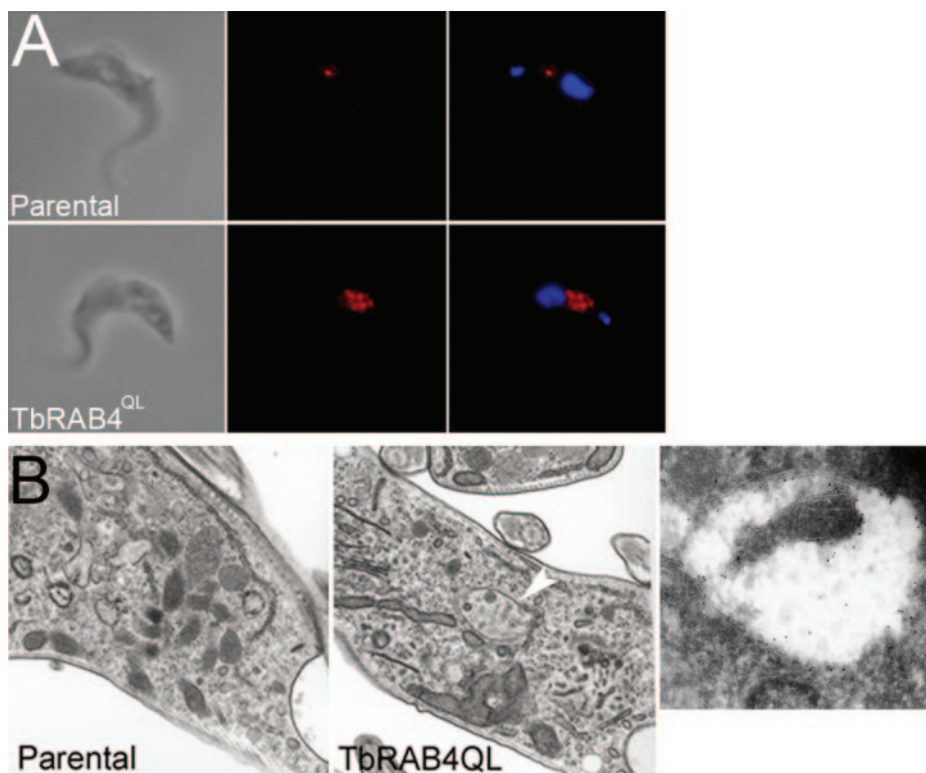


**FIG. 4. Expression of constitutively active TbRAB4<sup>QL</sup> leads to an enlargement of the p67 compartment.** A, expression of TbRAB4<sup>QL</sup> in bloodstream form *T. brucei*. Paraformaldehyde-fixed, permeabilized parental and mutant cells were stained with affinity-purified rabbit anti-TbRAB4 antibodies and visualized with Texas Red-conjugated goat anti-rabbit IgG. Cells are counterstained with DAPI to show the locations of the nucleus and kinetoplast. B, electron micrographs of parental and TbRAB4<sup>QL</sup>-expressing trypanosomes. A prominent multivesicular compartment (arrowhead) was observed in the majority of mutant cells. Similar effects were seen in two independently generated clones. Rightmost panel, immuno-electron microscopy staining of a multivesicular body with anti-p67 and 10 nm of gold. Note the gold particles within the lumen and around edge of the compartment. C, enhanced p67 signal in cells expressing TbRAB4<sup>QL</sup>. Fluorescence signal of p67 (green) in parental and TbRAB4<sup>QL</sup> cells, counterstained with DAPI (blue). Quantitation of fluorescence in at least 50 cells of each type revealed a significant ( $p < 0.001$ ) increase in intensity of signal in the TbRAB4<sup>QL</sup> cells. D, close physical association of TbRAB4 and p67 compartments. Parental and TbRAB4<sup>QL</sup> cells co-stained with rabbit anti-TbRAB4 (red) and with mouse anti-p67 mAb280 (green), counterstained with DAPI (blue). Note that p67 and TbRAB4 compartments are closely associated but do not colocalize in either cell type as the shapes of the structures are distinct. E, co-localization of internalized Con A with p67 in parental and mutant cells. Cells were allowed to take up biotinylated Con A for 30 min to label the lysosomal compartment before fixation and permeabilization. Biotin was detected with Texas Red-conjugated streptavidin. Cells were co-stained with mAb280 (green) and counterstained with DAPI (blue). Note the high degree of colocalization of signal in both cell types; in this case, the shapes of the labeled structures with the two markers are very similar and overlap.

transferrin release.<sup>2</sup> These data confirm that TbRAB4 does not play a direct or significant role in receptor-mediated endocytosis and recycling in *T. brucei*.

Upon endocytosis, fluid-phase markers are rapidly segregated from glycosylphosphatidylinositol-anchored proteins, with the latter being recycled directly to the surface via TbRAB11-positive vesicles and fluid-phase material transferred to the lysosome (18). To determine whether there is a role for TbRAB4 in fluid-phase endocytosis, induced TbRAB4 RNAi cells were allowed to accumulate Alexa Fluor 488-labeled dextran. Examination of cells showed a profound block in the accumulation of the fluorescent marker in cells lacking TbRAB4 expression (Fig. 2B). Quantitation of internalized fluorescence indicated a significant reduction of dextran levels in induced cells ( $p < 0.01$ ) (Fig. 2C). In light of the lack of an alteration in transferrin endocytosis and recycling, it is unlikely that the inhibition of fluid-phase accumulation is the result of nonspecific RNAi-induced toxicity. The data suggest that TbRAB4 is involved primarily in endocytic trafficking directing fluid-phase cargo toward the lysosome rather than in the recycling of surface proteins.

**TbRAB4 RNAi Disrupts the Lysosomal Compartment in *T. brucei***—To confirm a role for TbRAB4 in lysosomal traffick-

ing, the effect of TbRAB4 RNAi on the trypanosome lysosomal marker protein p67 was examined. Immunofluorescence revealed that the induction of double-stranded TbRAB4 RNA leads to p67 staining becoming increasingly dispersed over time, suggesting a progressive disruption of the lysosomal compartment or trafficking of p67 to the compartment (Fig. 3A). This appears to be a specific effect since RNAi of other Rab proteins or clathrin had no apparent effect on p67 localization despite severe cellular distortion (21, 23). To further investigate the effect of TbRAB4 RNAi on p67, the transport and processing of p67 was followed by a pulse-chase experiment. p67 is synthesized as a 100-kDa precursor protein in the endoplasmic reticulum. After *N*-glycan modification in the Golgi complex, the protein has an apparent molecular mass of 150 kDa. Subsequent trafficking to the lysosome leads to the appearance of major proteolytic fragments with apparent molecular masses of 75, 42, 32, and 28 kDa (33). Although there is evidence for transport of p67 to the lysosome via an indirect route involving export to the surface and subsequent retrieval, the bulk of the protein is thought to be delivered directly to the lysosome from the Golgi complex (33). In cells suppressed for TbRAB4, the initial steps of p67 processing, as judged by the disappearance of the 100-kDa species and concomitant appearance of the 150-kDa form, were normal (Fig. 3, B and C). Further, subsequent processing of the 150-kDa form occurs at

<sup>2</sup> B. S. Hall and M. C. Field, unpublished observations.

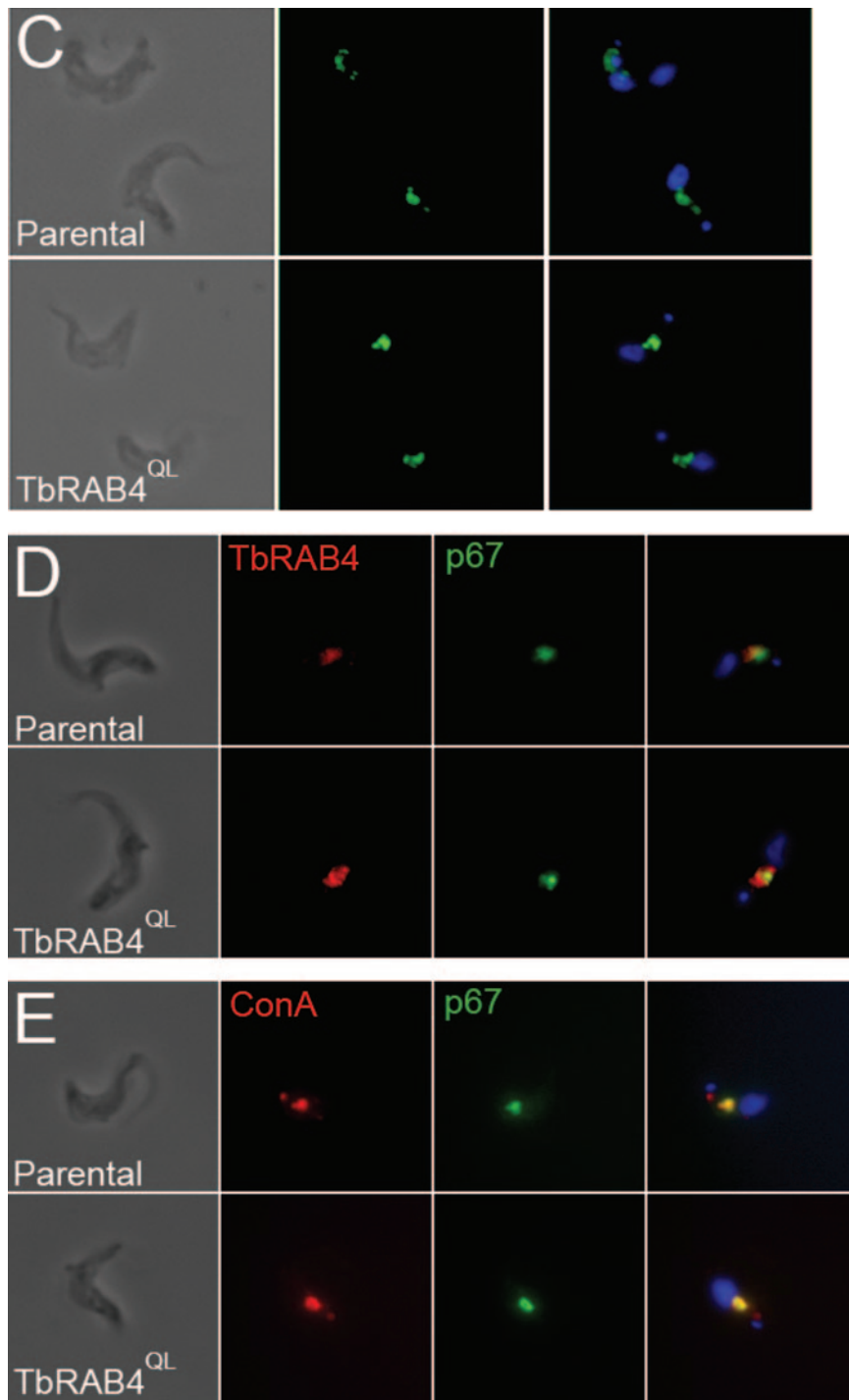


FIG. 4—continued

a similar rate in induced and uninduced cells. However, the levels of the low molecular weight products were reduced in cells suppressed for TbRAB4. The loss of these mature p67 forms may be due to mistargeting, altered degradation, or secretion or a combination of these factors. In any case, both immunofluorescence and p67 processing data together indicate that delivery of p67 to the lysosome is compromised in the absence of TbRAB4 expression, suggesting a defect in lysosomal targeting.

*Constitutively Active TbRAB4<sup>QL</sup> Induces Enlargement of the Lysosome*—The effects of TbRAB4 suppression on fluid-phase uptake and p67 localization and processing are suggestive of a function in regulation of lysosomal transport. To confirm this

role for TbRAB4, a constitutively active mutant, TbRAB4<sup>QL</sup>, possessing a Q67L mutation inhibiting GTPase activity, was expressed in trypanosomes (Fig. 4A). Cells expressing the mutant GTPase were morphologically normal at the light microscopy level. By electron microscopy, an increase in the number and size of multivesicular compartments was observed (Fig. 4B, mean diameter  $0.71 + 0.07 \mu\text{m}$  ( $n = 20$ ) when compared with  $0.47 + 0.05 \mu\text{m}$  ( $n = 15$ ) in parental cells,  $p < 0.02$ . Immunoelectron microscopy confirmed that the multivesicular compartment was positive for p67 (Fig. 4B, inset). By immunofluorescence, TbRAB4<sup>QL</sup> cells show enhanced p67 staining (Fig. 4C). Since total p67 synthesis and processing are largely unchanged in these cells (data not shown), this effect is probably

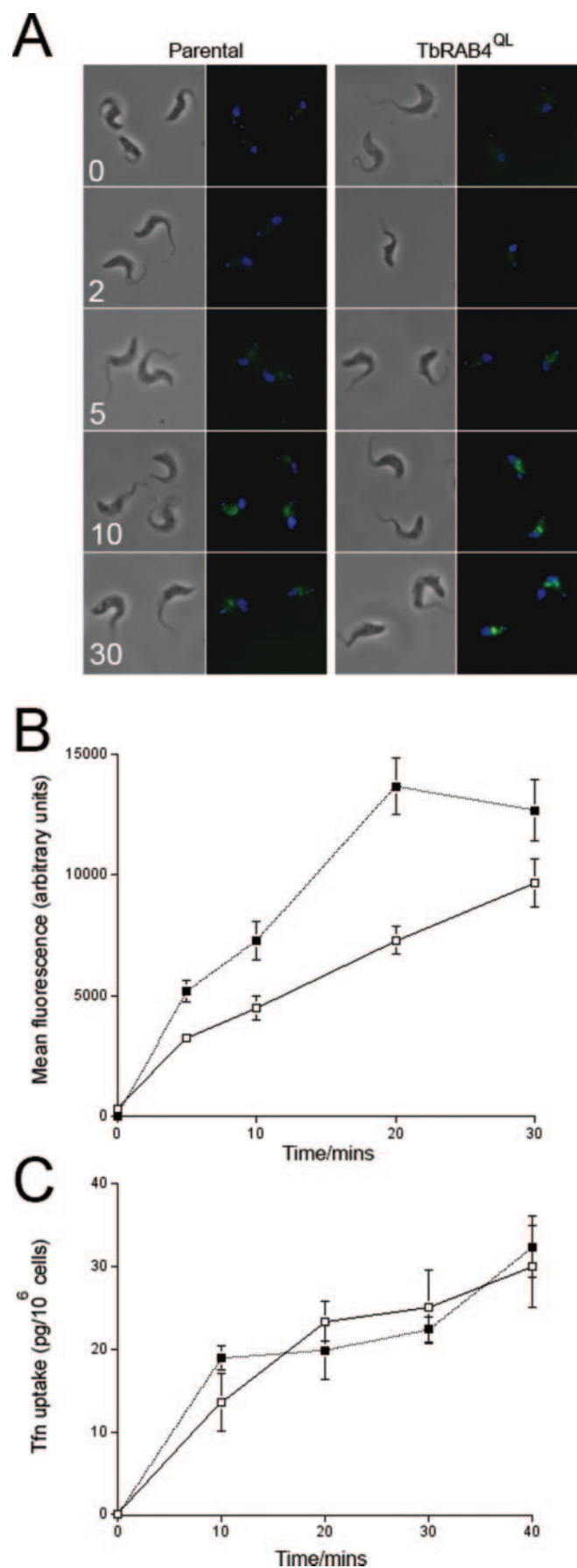


FIG. 5. Enhancement of fluid-phase but not transferrin (*Tfn*) uptake in TbRAB4<sup>QL</sup> cells. A, TbRAB4<sup>QL</sup> increases the rate of accumulation of a fluid-phase marker. Parental and TbRAB4<sup>QL</sup> cells were incu-

due to the increased size of the p67 compartment. Co-staining for p67 and TbRAB4 shows that TbRAB4 is closely associated with p67 but appears juxtaposed to the p67 compartment rather than colocalizing with the lysosomal marker (Fig. 4D). To verify that the enlarged multivesicular compartment was indeed the lysosome, TbRAB4<sup>QL</sup> cells were allowed to take up biotin-derivatized Con A for 30 min at 37 °C, conditions that label the lysosomal compartment. The bulk of internalized Con A colocalized with p67, in both wild type and mutant cells, confirming that the enlarged multivesicular body represents the terminal endocytic compartment and therefore represents the lysosome rather than an intermediate endosomal compartment (Fig. 4E).

*Fluid-phase Uptake Is Enhanced in Cells Expressing TbRAB4<sup>QL</sup>*—To further corroborate the evidence that TbRAB4 is involved in fluid-phase transport toward the lysosome, the uptake of Alexa Fluor 488 dextran was monitored in both the parental and the dominant active TbRAB4<sup>QL</sup>-expressing cells (Fig. 5). Internalized label was detectable earlier in the TbRAB4<sup>QL</sup> line, and the intensity of fluorescence was significantly higher than in parental cells (Fig. 5B). By contrast, expression of TbRAB4<sup>QL</sup> had no effect on the kinetics of <sup>125</sup>I-transferrin accumulation (Fig. 5C). These data are in agreement with the effects of RNAi on endocytosis and confirm a specific role for TbRAB4 in fluid-phase transport.

#### DISCUSSION

Rab4 has been implicated in a number of pathways in higher eukaryotes, including rapid recycling (presumed to be from the early endosome and downstream of Rab5 function), and also in degradative trafficking to the lysosome (3–7, 14, 15). Studies in a variety of cells support a differing emphasis on the precise function of Rab4 depending on the system under investigation, but important recent data have suggested that the level of integration between the major Rab proteins involved in endocytic transport (principally Rab4, -5, -7, and -11) is higher than previously suspected. For example Rab4, -5, and -11 can be visualized on distinct but contiguous subdomains of endosomal structures (34), whereas a number of effector molecules are capable of interacting with Rab4 and other endosomal Rab proteins (10). These issues potentially complicate the analysis of Rab proteins based on expression of mutant isoforms.

In *T. brucei*, a clear sequence orthologue of mammalian Rab4 is present, and previous work has localized this protein to structures closely associated with the early endosome (27). Attempts to use mutant isoforms of TbRAB4 to probe function were unsuccessful despite success with other trypanosomal Rab proteins (20, 28). Although this may reflect a trypanosomatid-specific configuration, it is also possible that Rab4 function is more subtle than, for example, Rab11, and that overexpression of mutant isoforms does not fully reveal the function of Rab4. As conditional gene knockout technology is cumbersome in higher eukaryotes, ablation of TbRAB4 expression has not been attempted, but using trypanosomes, we were able to ben-

ated for various times with 5 mg ml<sup>-1</sup> Alexa Fluor 488 dextran 10000 (green). Cells were fixed in 4% paraformaldehyde, adhered to poly-L-lysine slides, counterstained with DAPI (blue), and examined immediately. B, quantitation of dextran uptake. Parental (open squares) and TbRAB4<sup>QL</sup> (closed squares) cells were incubated with fluorescent dextran as described above, and signal intensity was quantified for at least 30 cells for each cell type at each time point. Data points represent mean ± S.E. Results presented are typical of three independent experiments. C, TbRAB4<sup>QL</sup> has no effect on the uptake of transferrin. The incorporation of <sup>125</sup>I-labeled transferrin into parental BSF (open squares) and TbRAB4<sup>QL</sup> cells (closed squares) at various time points is shown. Each point represents the mean of duplicate determinations ± range. Similar results were obtained in multiple experiments.

efit from the comparative simplicity of RNA interference for suppression. The work presented here suggests that TbRAB4 is exclusively involved in fluid-phase lysosomal transport and has no role in receptor-mediated uptake and recycling.

Our first major conclusion is that TbRAB4 is essential but that there is no evidence for a direct role in endocytosis or recycling. Previous studies have shown that RNAi of proteins involved in early endocytosis, specifically clathrin, actin, and TbRAB5, is rapidly lethal and is associated with the appearance of an enlarged flagellar pocket, which presumably arises due to imbalance between the removal and addition of membrane to the surface (21–23). Despite the closeness of the physical locations of TbRAB4 and TbRAB5A, cells lacking TbRAB4 rarely display this distinctive phenotype, and progression to cell death is much slower, implying a function for TbRAB4 in distinct pathways. This assumption is supported by the failure of either TbRAB4 RNAi or TbRAB4<sup>QL</sup> to impact on transferrin uptake and is concordant with previous single turnover studies (20).

The second major finding is the clear implication of TbRAB4 in delivery of cargo to the lysosome, as illustrated for both the accumulation of fluid-phase cargo using fluorescent dextran and the delivery of the lysosomal protein p67. Additionally, overexpression of TbRAB4<sup>QL</sup> leads to an enlargement of the later portions of the endocytic system, also consistent with a role in lysosomal targeting. The kinetics of p67 synthesis and transport do not change dramatically in the mutant cells. Rather, the size and/or the stability of the lysosome appear to be altered, leading to a decrease in the accumulation of p67 proteolytic products and dissipation of p67 staining in the case of TbRAB4 RNAi and an increase in p67 staining and physical size of the p67 compartment when TbRAB4 activity is enhanced. It seems most likely that, rather than acting directly on the lysosome, TbRAB4 mediates these changes by controlling the volume of traffic directed toward the lysosome.

It is somewhat surprising that alterations in TbRAB4 activity that have a profound effect on the lysosome do not appear to affect transferrin turnover. VSG and the transferrin receptor are cycled back to the surface via TbRAB11-positive vesicles either directly or via the late endosome, but the route taken by internalized anti-VSG immunoglobulin and transferrin is less clear. Both are extensively degraded after internalization, but their export is still TbRAB11-dependent (20, 24). It is possible that the bulk of anti-VSG immunoglobulin and transferrin follows their respective binding partners and is degraded in the late endosomes, bypassing the lysosome altogether. Transferrin is detectable in the lysosome, especially in the presence of protease inhibitors (25), but this may represent a small fraction of the total internalized protein. Alternatively, it is possible that all transferrin is transported to the lysosome and that TbRAB11 controls recycling from the lysosome in addition to regulating the more rapid recycling pathways. This model appears to be in conflict with the data presented here since TbRAB4 RNAi disrupts the lysosome and lysosomal transport without altering the uptake of transferrin or export of its degradative products. Nevertheless, receptor-bound ligands and fluid-phase cargo are clearly transported independently and, in the absence of a functional lysosomal compartment, exit via TbRAB11 vesicles may represent an alternative route for transferrin that is not available for dextran and may therefore lessen the impact of impaired lysosomal transport on transferrin uptake and degradation. As well as altering recycling patterns, expression of mutant TbRAB11 proteins affects the degree of transferrin degradation (20), suggesting some reciprocity between recycling and degradative path-

ways. Our data also strongly suggest that TbRAB11 alone controls recycling in bloodstream trypanosomes. TbRAB4 may have a minor role in recycling of membrane in the insect stage,<sup>3</sup> but significantly, TbRAB11 is expressed at very low levels in this life stage, and surface proteins are not subject to the continuous rapid recycling seen in the bloodstream forms (24).

Overall, the trypanosomal endocytic system is very similar to that of metazoans, with the notable exceptions that endocytosis appears to be exclusively clathrin-mediated and dynamin- and adaptin-independent (21, 35, 36). A very high rate of recycling in this system may have selected for a streamlined system, and it is possible that in trypanosomatids, any role that Rab4 originally played in recycling may have been lost. Early studies on the function of Rab4 indicate a role in recycling of the mammalian transferrin receptor, and subsequent experiments using overexpression of wild type and Rab4<sup>QL</sup> mutants confirm this (*e.g.* 3). In addition, an observation common to these studies is an altered morphology of the early endosome and a shift in the transferrin receptor distribution to a more predominant surface location, fully consistent with an influence on recycling. Additional data in the mammalian system suggest a minimal role in endocytosis but a significant function in degradation of low density lipoprotein and epidermal growth factor (14). Recently, two effectors for Rab4 have been identified. One of these, rabip4', also interacts with Rab5 and appears to be predominantly involved in recycling pathways (4). By contrast, a second Rab4 effector, CD2AP/MS, appears to function in a degradative pathway and does not appear to play any role in transferrin receptor recycling (15). These studies, taken together with the data presented here for trypanosomes, indicate that Rab4 has the potential to function in both recycling and degradative pathways. The precise emphasis is likely dictated by effector molecules rather than by the GTPase itself. This has interesting consequences for the evolution of the endocytic system, and in particular, suggests that it is naive to attempt to make precise predictions of function based solely on the presence or absence of a particular Rab subfamily; knowledge of the effector molecules cooperating with the Rab protein is essential.

*Acknowledgments*—We thank George Cross for the 90-13 cell line, John Donelson for the p2T7<sup>Ti</sup> plasmid, and Jay Bangs for anti-p67 and anti-TbBiP antibodies.

#### REFERENCES

1. Maxfield, F. R., and McGraw, E. (2004) *Nat. Rev. Mol. Cell. Biol.* **5**, 121–132
2. Zerial, M., and McBride, H. (2001) *Nat. Rev. Mol. Cell. Biol.* **2**, 107–117
3. van der Sluijs, P., Hull, M., Webster, P., Male, P., Goud, B., and Mellman, I. (1992) *Cell* **70**, 729–740
4. Fouraux, M. A., Deneka, M., Ivan, V., van der Heijden, A., Raymackers, J., van Suylekom, D., van Venrooij, W. J., van der Sluijs, P., and Pruijn, G. J. (2004) *Mol. Biol. Cell* **15**, 611–624
5. Seachrist, J. L., and Ferguson, S. S. (2003) *Life Sci.* **74**, 25–35
6. Roberts, M., Barry, S., Woods, A., van der Sluijs, P., and Norman, J. (2001) *Curr. Biol.* **11**, 1392–1402
7. Wissel, H., Lehfeldt, A., Klein, P., Muller, T., and Stevens, P. A. (2001) *Am. J. Physiol.* **281**, L345–L360
8. Vitale, G., Rybin, V., Christoforidis, S., Thornqvist, P., McCaffrey, M., Stenmark, H., and Zerial, M. (1998) *EMBO J.* **17**, 1941–1951
9. Wallace, D. M., Lindsay, A. J., Hendrick, A., and McCaffrey, M. W. (2002) *Biochem. Biophys. Res. Commun.* **292**, 909–915
10. de Renzis, S., Sonnichsen, B., and Zerial, M. (2002) *Nat. Cell Biol.* **4**, 124–133
11. Lindsay, A. J., Hendrick, A. G., Cantalupo, G., Senic-Matuglia, F., Goud, B., Bucci, C., and McCaffrey, M. W. (2002) *J. Biol. Chem.* **277**, 12190–12199
12. Shirakawa, R., Yoshioka, A., Horiuchi, H., Nishioka, H., Tabuchi, A., and Kita, T. (2000) *J. Biol. Chem.* **275**, 33844–33849
13. Imamura, T., Huang, J., Usui, I., Satoh, H., Bever, J., and Olefsky, J. M. (2003) *Mol. Cell. Biol.* **23**, 4892–4900
14. McCaffrey, M. W., Bielli, A., Cantalupo, G., Mora, S., Roberti, V., Santillo, M., Drummond, F., and Bucci, C. (2001) *FEBS Lett.* **495**, 21–30
15. Cormont, M., Meton, I., Mari, M., Monzo, P., Keslair, F., Gaskin, C., McGraw,

<sup>3</sup> B. S. Hall and M. C. Field, manuscript in preparation.

- T. E., and Le Marchand-Brustel, Y. (2003) *Traffic* **4**, 97–112
16. Morgan, G. W., Hall, B. S., Denny, P. W., Carrington, M., and Field, M. C. (2002) *Trends Parasitol.* **18**, 491–496
  17. Grünfelder, C. G., Engstler, M., Weise, F., Schwarz, H., Stierhof, Y. D., Morgan, G. M., Field, M. C., and Overath, P. (2003) *Mol. Biol. Cell* **14**, 2029–2040
  18. Engstler, M., Thilo, L., Weise, F., Grünfelder, C., Schwarz, H., and Boshart, M. (2004) *J. Cell Sci.* **117**, 1105–1115
  19. Landfear, S. M., and Ignatushchenko, M. (2001) *Mol. Biochem. Parasitol.* **115**, 1–17
  20. Pal, A., Hall, B., Jeffries, T., and Field, M. C. (2003) *Biochem. J.* **374**, 443–451
  21. Allen, C. L., Goulding, D., and Field, M. C. (2003) *EMBO J.* **22**, 4991–5002
  22. Garcia-Salcedo, J. A., Perez-Morga, D., Gijon, P., Dilbeck, V., Pays, E., and Nolan, D. (2004) *EMBO J.* **23**, 780–789
  23. Hall, B., Allen, C. L., Goulding, D., and Field, M. C. (2004) *Mol. Biochem. Parasitol.*, in press
  24. Jeffries, T. R., Morgan, G. W., and Field, M. C. (2001) *J. Cell Sci.* **114**, 2617–2626
  25. Steverding, D., Stierhof, Y. D., Fuchs, H., Tauber, R., and Overath, P. (1995) *J. Cell Biol.* **131**, 1173–1182
  26. Ackers, J. P., Dhir, V., and Field, M. C. (2004) *Mol. Biochem. Parasitol.*, in press
  27. Field, H., Farjah, M., Pal, A., Gull, K., and Field, M. C. (1998) *J. Biol. Chem.* **273**, 32102–32110
  28. Pal, A., Hall, B. S., Nesbeth, D. N., Field, H. I., and Field, M. C. (2002) *J. Biol. Chem.*, **277**, 9529–9539
  29. LaCount, D. J., Bruse, S., Hill, K. L., and Donelson, J. E. (2000) *Mol. Biochem. Parasitol.* **111**, 67–76
  30. Kelley, R. J., Brickman, M. J., and Balber, A. E. (1995) *Mol. Biochem. Parasitol.* **74**, 167–178
  31. Bangs, J. D., Uyetake, L., Brickman, M. J., Balber, A. E., and Boothroyd, J. C. (1993) *J. Cell Sci.* **105**, 1101–1113
  32. Alexander, D. L., Schwartz, K. J., Balber, A. E., and Bangs, J. D. (2002) *J. Cell Sci.* **115**, 3253–3263
  33. Steverding, D. (1998) *Parasitol. Res.* **84**, 59–62
  34. Sonnichsen, B., De Renzis, S., Nielsen, E., Rietdorf, J., and Zerial, M. (2000) *J. Cell Biol.* **149**, 901–914
  35. Morgan, G. W., Allen, C. L., Jeffries, T. R., Hollinshead, M., and Field, M. C. (2001) *J. Cell Sci.* **114**, 2605–2615
  36. Morgan, G. W., Hall, B. S., Denny, P. W., Field, M. C., and Carrington, M. (2002) *Trends Parasitol.* **18**, 540–546